STEEL FIBRES FOR THE SHEAR RESISTANCE OF HIGH STRENGTH CONCRETE BEAMS

Simao P.F. Santos [(1)], Joaquim A.O. Barros [(1)] and Lúcio A.P.Lourenço [(1)]

(1) School of Engineering, University of Minho, Portugal

Abstract

Available research on the use of steel fibres to increase the shear resistance of concrete structures shows that the effectiveness of this type of reinforcement increases with the increase of the concrete compressive strength, as long as the fibre rupture is avoided. Experimental research has also indicated that the effectiveness of the fibre reinforcement for the shear resistance is more pronounced in shallow beams than in deep beams. In terms of analytical research, some models have been proposed and, recently, RILEM TC 162 TDF recommended an analytical approach for the prediction of the fibre reinforcement contribution in terms of shear resistance of concrete beams.

The present work has the purpose to contribute for this topic, discussing the performance of RILEM TC 162 TDF approach, by using the results obtained in an experimental program composed of three point bending tests with shallow beams of high strength concrete (HSC).

Six different HSC compositions were developed, varying the dosage of steel fibres (0, 60 and 75 kg/m^3) and concrete strength class. The experimental program also included tests to characterize the flexural behaviour of the developed high strength steel fibre reinforced concrete (HSSFRC).

Using the force-deflection relationships obtained in the three point-notched beam bending tests, and performing an inverse analysis, the values of the fracture mode I parameters of the HSSFRC were determined. These values were used on the numerical simulation of the tests carried out with HSSFRC beams failing in shear, under the framework of the material nonlinear finite element analysis, in order to evince the influence of using a softening constitutive law for modeling the crack shear sliding.

In the present work, the experimental program and the numerical research are described, and the main results are presented and discussed.

1. INTRODUCTION

Available research shows that steel fibre reinforcement, in certain circumstances, can be used as the unique reinforcement for the shear resistance of concrete beams, and, more currently, can replace a certain percentage of steel stirrups, with technical and economic advantages [1]. In fact, Casanova [2] concluded that steel fibres may substitute significant percentages of steel stirrups, especially when high strength concrete (HSC) is used, once the fibre reinforcement mechanisms are more effectively mobilized. This research also evinced that the beam depth has a remarkable influence on the fibre reinforcement performance, since as higher was the beam depth as less effective was the steel fibre reinforcement.

In the present work, high strength steel fibre reinforced concrete (HSSFRC) compositions were designed to provide an effective medium for the fibre reinforcement, in order to compet with steel stirrups for the shear reinforcement of HSC laminar structures. For the characterization of the post-cracking flexural behaviour, three point notched-beam bending tests were carried out according to the RILEM TC 162-TDF recommendations [3]. Performing an inverse analysis with the obtained force-deflections curves, the fracture mode I parameters of the HSSFRC were obtained. These values were used to characterize the crack opening component of a smeared crack constitituve model, which can also simulate the crack sliding component with the current concept of shear retention factor or with the use of a crack-shear softening diagram. The influence of these two alternatives for modeling the crack shear behaviour, on the response of the tested beams is analyzed in the numerical session of the present paper.

2. EXPERIMENTAL PROGRAM

2.1 Compositions, series, specimens, support, load and monitoring conditions

Using three dosages of steel fibers (Q_f), 0, 60 and 75 kg per m^3 of concrete, six different compositions of HSC were developed (see Table 1), grouped in two main series, the first one designed to have an average compressive strength of 50 MPa (in fact, as Table 3 shows, the compressive strength varied from 41 to 48 MPa, at 14 days), and the second one to attain an f_{cm} of 70 MPa (an f_{cm} was around 66 MPa was obtained – see Table 3). DRAMIX® RC 80/60 BN hooked ends steel fibres were used in these compositions. These fibres have a length, l_f , of 60 mm, a diameter, d_f, of 0.75 mm, an aspect ratio (l_f / d_f) of 80 and a yield stress of 1100 MPa.

For each composition three cylinders (150 mm diameter and 300 mm height), three cubes (150 mm edge) and four prismatic specimens (600×150×150 mm^3) were casted and tested to evaluate the compression and bending behavior of the developed HSSFRC. To evaluate the influence of the fibre percentage in the shear resistance of HSC elements, three point bending tests with beams (800×170×150 mm^3 – length, width and depth) were carried out (distance between supports equal to 720 mm). For each composition, four beams were casted, two of them including ordinary longitudinal reinforcement (2Φ20 at bottom surface, with a concrete cover of 20mm, and 2Φ6 at top surface -just constructive rebar-, with a concrete cover of 20mm) and two without ordinary reinforcement, to serve as reference. A total of twenty-four slab strips were casted and tested. Three LVDTs supported on a Japenese Yoke, one placed at the loaded section (intermediate section of the beam), and the others at the middle of each shear span, were used.

Table 1: Compositions of HSSFRC used in the present work (per m^3 of concrete)

Series	*Cement (kg)*	*Water (dm^3)*	*Limestone Filler (kg)*	*16/20 Agg. (kg)*	*5/10 Agg. (kg)*	*2/5 Agg. (kg)*	*Fine Sand (kg)*	*SP (dm3)*	*Steel Fibres (kg)*
fcm50_NoFibres	300.0	120.46	114.0	308.9	309.2	503.4	587.0	5.36	0
fcm50_FC60	300.0	120.46	228.0	294.3	294.5	457.6	533.6	7.01	60
fcm50_FC75	300.0	120.46	228.0	286.1	286.5	448.9	560.6	7.01	75
fcm70_ NoFibres	400.0	114.00	200.0	303.1	303.3	471.3	549.6	7.84	0
fcm70_FC60	400.0	114.00	342.0	282.5	282.7	439.3	512.3	10.65	60
fcm70_FC75	400.0	114.00	342.0	266.1	266.5	417.5	521.3	10.65	75

2.2 Main obtained results and discussion

The load-central deflection curves obtained from the three point bending tests carried out with the shallow beams with ordinary longitudinal reinforcement are present in Figure 1. Table 2 includes the force at a deflection corresponding to the serviceability limit state (L/400 with L being the span length in mm), F_{ELUt}, as well as the maximum force, F_{max}, registered in the tests. Each curve is the average of two tests.

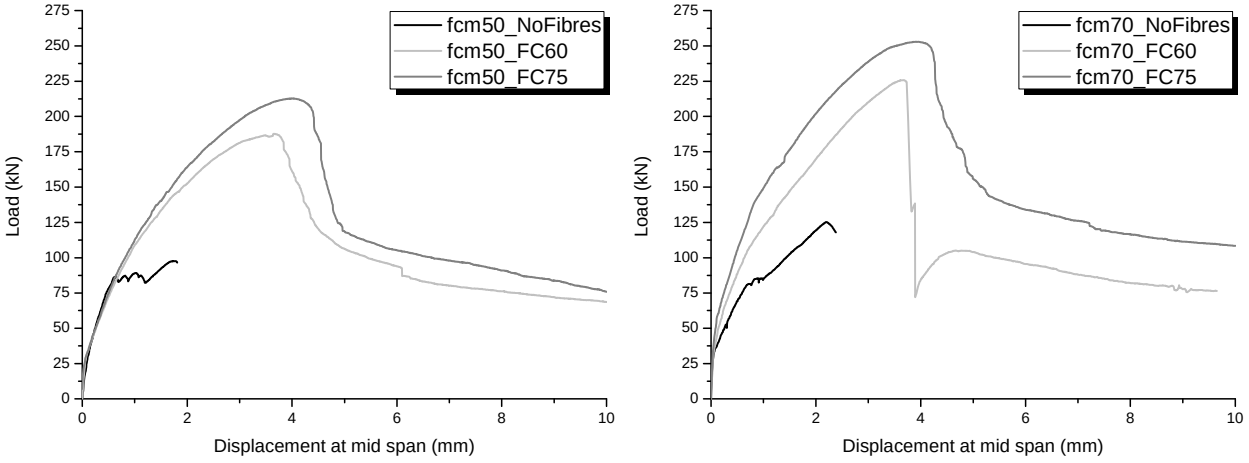

a) f_{cm} = 50 MPa b) f_{cm} = 70 MPa

Figure 1: Load-mid span deflection curves for the series with ordinary longitudinal reinforcement

To estimate the contribution of fibre reinforcement at serviceability and at ultimate limit states, the values of the following ratio were determined

$$I_F = \frac{F_{Qf} - F_{ref}}{F_{ref}} \times 100 \quad (1)$$

where F_{Qf} is the force of the HSSFRC beam and F_{ref} is the force of the corresponding beam without steel fibres. The obtained values for I_F are indicated in-between round brackets, in Table 2, from which it can be concluded that fibre reinforcement provided a contribution for the load carrying capacity of the beams, at deflection corresponding to the serviceability limit state analysis, ranging from 43% up to 72%, while for the maximum load the fibre reinforcement effectiveness varied from 80% up to 118%. A part the case of F_{ELUt} for the beams reinforced with 75 kg/m^3 of fibres, it is verified that for the same content of fibres, the increase percentage in terms of F_{ELUt} and F_{max} decreased with the increase of the concrete strength. Two reasons might justify this behaviour: i) The released energy at concrete fracture increases with the increase of concrete strength. If the number of fibres that are crossing an initiating crack is the same for specimens of distinct concrete strength classes, the damages introduced in the fibre-concrete bond properties during the stress transference from concrete to fibres augment with the increase of concrete strength, resulting a detrimental effect in terms of fibre reinforcement mechanisms; ii) The possibility of the occurrence of fibre rupture increases with the increase of the concrete strength, which has a detrimental effect in terms of load carrying capacity and energy dissipation.

Table 2: Values for the F_{ELUt} and F_{max} (in brackets is indicated the increase percentage values, I_F)

Series	F_{ELUt}			F_{max}		
	$Q_f = 0$ kg/m^3	$Q_f = 60$ kg/m^3	$Q_f = 75$ kg/m^3	$Q_f = 0$ kg/m^3	$Q_f = 60$ kg/m^3	$Q_f = 75$ kg/m^3
fcm50	97.35	146.06 (50%)	154.83 (59%)	97.66	187.50 (92%)	212.73 (118%)
fcm70	112.10	160.29 (43%)	192.36 (72%)	125.23	225.82 (80%)	252.90 (102%)

2.2 Failure modes

As Figure 2 shows all reinforced tested beams failed in shear. The number of flexural cracks formed up to the ocurrence of the shear failure crack increased with the increase of the content of steel fibres. Furthermore, it is visible that the inclination of the shear failure crack (angle of the shear crack plan with the beam longitudinal axis) decreased with the increase of the content of fibres, which justifies the resulting benefits of fibre reinforcement, since larger area of crack, bridged by fibres, is available, and more favorable inclination of the fibre resisting tensile force is moblized for the shear resistance. Moreover, due to the crack opening arrestment offered by fibres briding the shear crack plans, a diffuse crack pattern occurred in the vicinity of the shear failure crack, contributing for the increase of energy dissipation and for the more ductile failure mode observed in HSSFRC beams, in comparison to HSC beams.

a) b) c)

Figure 2: Crack Pattern in *f*cm50 series: a) without fibres, b) 60 kg/m^3 and c) 75 kg/m^3 of fibres

3. RILEM TC 162-TDF APPROACH

According to the formulation proposed by RILEM TC 162-TDF committee [3], the shear resistance of a concrete element reinforced with steel stirrups, steel fibres and ordinary longitudinal reinforcement is given by:

$$V_{Rd3} = V_{cd} + V_{fd} + V_{wd} \tag{2}$$

where V_{cd} represents the concrete contribution for the shear resistance:

$$V_{cd} = \left[0.12\, k \left(100\, \rho_\ell\, f_{ck}\right)^{\frac{1}{3}} + 0.15\, \sigma_{cp} \right] b_w\, d \ \text{[N]} \tag{3}$$

$$k = 1 + \sqrt{\frac{200}{d}} \ (d \text{ in mm}) \text{ and } k \le 2, \tag{4}$$

$$\rho_\ell = \frac{A_{s\ell}}{b_w\, d} \le 2\% \tag{5}$$

with $A_{s\ell}$ being the cross section area of the tensile longitudinal reinforcement, b_w is the minimum width of the web cross section, d is the effective depth of the cross section,

$$\sigma_{cp} = \frac{N_{sd}}{A_c} \text{ [N/mm}^2\text{]} \quad (6)$$

where N_{sd} [N] is the axial force due to applied external load (compression is assumed positive) and A_c [mm^2] is the area of the cross section. The contribution of steel fibres, V_{fd}, is determined by

$$V_{fd} = 0.7\, k_f\, k_l\, \tau_{fd}\, b_w\, d \text{ [N]} \quad (7)$$

where k_f is a factor taking the contribution of the flanges in a T cross section,

$$k_f = 1 + n\left(\frac{h_f}{b_w}\right)\left(\frac{h_f}{d}\right) \leq 1.5 \quad (8)$$

with h_f [mm] and b_f [mm] being the heigh and width of the flanges, respectively, and

$$n = \frac{b_f - b_w}{h_f} \leq \min\left(3;\ \frac{3\, b_w}{h_f}\right) \quad (9)$$

The fibre reinforcement contribution is simulated by τ_{fd}, that can be determined by:

$$\tau_{fd} = 0.12\, f_{eqk,3} \text{ [N/mm}^2\text{]} \quad (10a)$$

or, alternativelly,

$$\tau_{fd} = 0.12\, f_{Rk,4} \text{ [N/mm}^2\text{]} \quad (10b)$$

where $f_{eqk,3}$ and $f_{Rk,4}$ are the characteristic values of the equivalent and the residual flexural tensile strength parameters determined according to the recomendations of RILEM TC 162-TDF [3].

In (2), V_{wd} represents the contribution of steel stirrups or inclined bars,

$$V_{wd} = \frac{A_{sw}}{s} 0.9\, d\, f_{ywd} \left(1 + \cot g\alpha\right) \sin\alpha \text{ [N]} \quad (11)$$

where A_{sw} is the cross section area of the arms of the steel stirrup, s is the distance between consecutive stirrups, f_{ydw} is the design yield stress of the stirrup and α is the inclination of the shear failure crack (assumed 45°). In the present experimental program V_{wd}=0.

Applying the RILEM approach, the values of the fibre reinforcement contribution are included in Table 3. The values of $f_{eqk,3}$ and $f_{Rk,4}$ used in (10) were determined from the force-deflection curves registered in the three point notched beam bending tests (see Fig. 5).

From Table 3 it can be concluded that RILEM approach provided a global shear design safety factor higher than 2.0. Furthermore, this safety factor increased with the increase of the content of fibres, and was significantly higher in fibrous RC beams than in RC beams without fibres. For the developed compositions, the option for the $f_{Rk,4}$ in detriment of $f_{eqk,3}$ led to a more conservative predictions in terms of the shear resistance.

Table 3: Contribution of steel fibres to the concrete shear resistance.

Series	*fcm* (kN)	*fck* (kN)	*Vcd* (kN)	$\tau_{fd,1}$ [(1)] (MPa)	$\tau_{fd,2}$ [(2)] (MPa)	V_{fd} [(1)] (kN)	V_{fd} [(2)] (kN)	V_{Rd} [(1)] (kN)	V_{Rd} [(2)] (kN)	SF,1 [(3)]	SF,2 [(3)]
fcm50_NoFibres	41.74	33.74	26.35	-	-	-	-	26.35	-	1.85	-
fcm50_FC60	46.58	38.58	27.56	1.06	0.92	15.19	13.11	42.76	40.67	2.20	2.31
fcm50_FC75	48.10	40.10	27.92	1.42	1.24	20.34	17.65	48.25	45.57	2.21	2.34
fcm70_ NoFibres	66.39	58.39	31.64	-	-	-	-	31.64	-	1.98	-
fcm70_FC60	65.73	57.73	31.52	1.47	1.25	21.02	17.81	52.44	49.33	2.14	2.28
fcm70_FC75	66.08	58.08	31.59	1.71	1.55	24.39	22.13	55.98	53.72	2.25	2.35

[(1)] using $\tau_{fd} = 0.12\, f_{eqk,3}$ [N/mm^2]; [(2)] using $\tau_{fd} = 0.12\, f_{Rk,4}$ [N/mm^2]; [(3)] Ratio between V_{exp} and V_{Rd}[(1)] (or V_{Rd}[(2)]).

4. NUMERICAL SRATEGY

4.1 Introduction

Previous research indicated that fracture mode I propagation can be simulated using a tri-linear softening diagram (Figure 3b), whose parameters (mode I fracture energy, G_f^I, and values of $\varepsilon_{n,i}^{cr}$ and $\sigma_{n,i}^{cr}$ that define the shape of the softening diagram) can be obtained performing inverse analysis with the force-deflection data registered in three-point notched beam bending tests carried out according to the RILEM TC 162-TDF recommendations [4]. To simulate the crack shear sliding, a shear retention factor (β) is currently used. With this model the increment of shear stress ($\Delta\tau_{nt}^{cr}$) transfer between the crack planes decreases with the increase of the crack normal strain (ε_n^{cr}), according to an assumed relationship between β and ε_n^{cr}, like the following one: $\beta = \left(1-\varepsilon_n^{cr}/\varepsilon_{n,u}^{cr}\right)^p$, where *p* defines the decrease level of β with the increase of the crack normal strain [5]. In most structures assumed as behaving in plane stress state this strategy provides simulations with reasonable accuracy. Exceptions occur in structures that fail by the formation of a critical shear crack. For these cases, to simulate the structural softening with high accuracy it is required the adoption of a softening crack shear stress vs. crack shear strain relationship, like the one represented in Figure 3c, where τ_p^{cr} is the concrete shear strength and G_f^{II} is the mode II fracture energy. In the performed analysis it was assumed the same crack band width (l_b) for either the fracture mode I and fracture mode II diagrams. In order to obtain results indepement of the finite mesh refinement, the value of l_b was assumed equal to the square root of the area of the corresponding GP.

4.2 Inverse analysis

To assess the fracture mode I concrete fracture parameters an inverse analysis was performed, evaluating the values of the σ_i and w_i of the $\sigma - w$ diagram (see Figure 4) that fit the experimental $F-\delta$ curves obtained in the three point notched beam bending tests, with the minimum error of the parameter $err = \left|A_{F-\delta}^{\exp} - A_{F-\delta}^{num}\right| \Big/ A_{F-\delta}^{\exp}$ where $A_{F-\delta}^{\exp}$ and $A_{F-\delta}^{num}$ are the areas below the experimental and the numerical $F-\delta$ curve, respectively. Figure 5 shows the finite element mesh used. 2D line interface finite elements were located in the specimen's symmetry axis [8]. In the remaining parts of the specimen linear eight-node Serendipity plane-stress elements were used.

Gauss-Lobatto integration scheme [6] with three integration points (IP) was used for the 2D line interface finite elements, while Gauss-Legendre integration scheme with 2×2 IP was used for the eight-node elements. The values of the concrete Young's Modulus, E_c, considered in the analysis are indicated in Table 4.

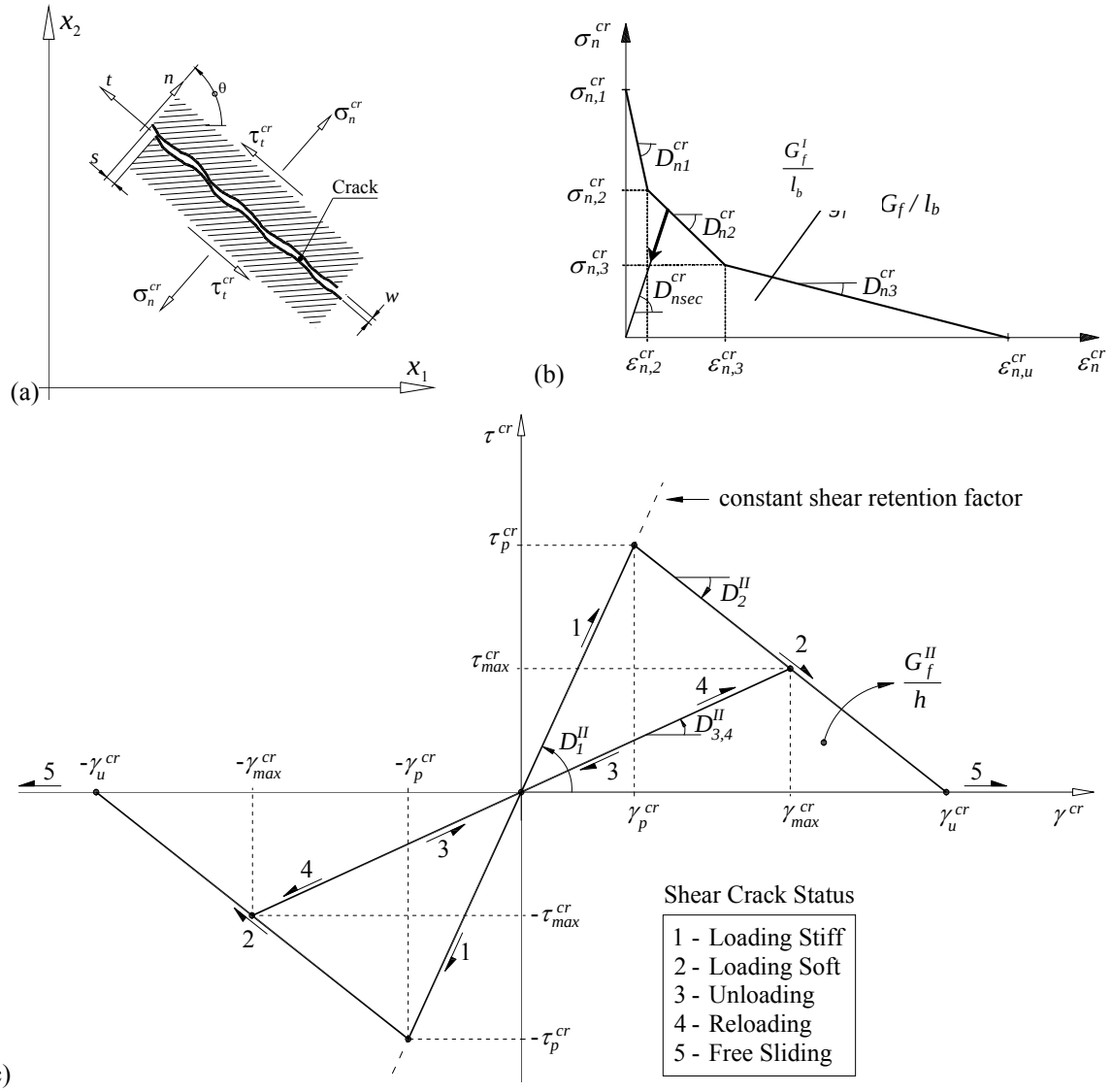

Figure 3: (a) Crack stress components, relative displacements and local coordinate system of the crack , (b) tri-linear normal stress - normal strain diagram to simulate the fracture mode I crack propagation; and (c) bi-linear shear stress-shear strain diagram to simulate the fracture mode II crack sliding.

The adequacy of the numerical strategy adopted is shown in Figure 6, revealing that the proposed trilinear $\sigma - w$ diagram is capable of predicting, with enough accuracy, the post-cracking behaviour of the tested specimens. Similar performances were obtained in the remaining series of tests.

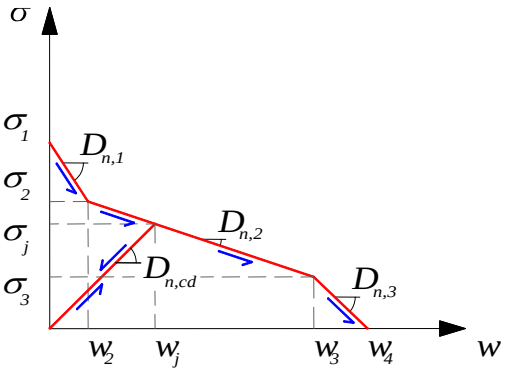

Figure 4: Stress-crack opening diagram

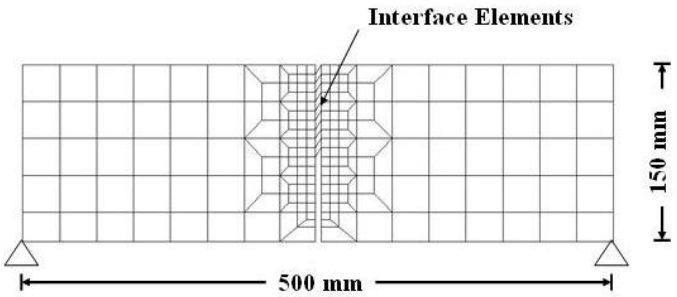

Figure 5 : Finite element mesh adopted in the inverse analysis

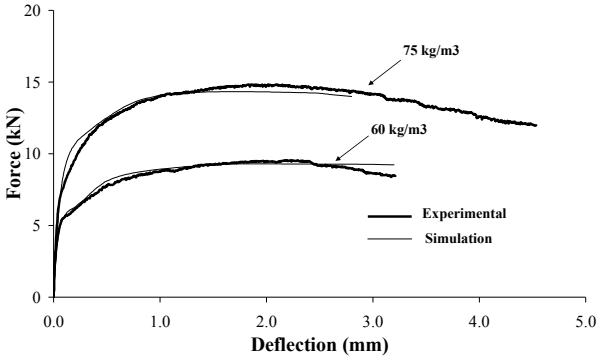

a) f_{cm} = 50 MPa

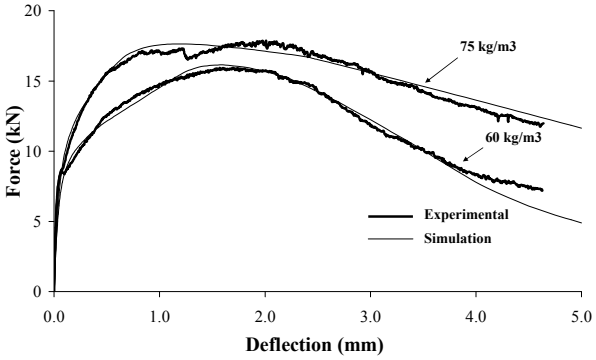

b) f_{cm} = 70 MPa

Figure 6: force-deflection curves of the nothced beam bending tests: comparison between experimental and inverse analysis results

4.3 Simulations of the beams' tests

The performance of the crack shear softening model was assessed by the simulation of the experimental tests with beams failing in shear. A finite element mesh of 406 plane stress elements of 8 nodes, with a Gauss-Legendre 2×2 integration scheme, was used in these simulations. The steel bars were simulated by perfect bonded two nodes elements, with 2 IP. Due to the structural symmetry of the beams, only half part of the beam was simulated. The values of the fracture mode I parameters of the smeared crack consitutive model, used in the simulations, and included in Table 4, were directly derived from the inverse analysis.

Table 4: Values of the parameters of the constitutive model used in the simulations

Series	Tri-linear tension softening diagram							Softening crack shear stress-strain diagram		
	E_c (N/mm²)	$\sigma_{n,1}^{cr}$ (N/mm²)	ξ_1	α_1	ξ_2	α_2	G_f^I (N/mm)	τ_p^{cr} (N/mm²)	G_f^{II} (N/mm)	β
fcm50_FC60	37045	1.90	0.002	0.950	0.035	1.350	3.200	3.40	5.20	0.5
fcm50_FC75	39014	3.50	0.001	0.950	0.044	1.200	5.140	3.00	3.10	0.5

$\alpha_1 = \sigma_{n,2}^{cr} / \sigma_{n,1}^{cr}$, $\alpha_2 = \sigma_{n,3}^{cr} / \sigma_{n,1}^{cr}$, $\xi_1 = \varepsilon_{n,2}^{cr} / \varepsilon_{n,u}^{cr}$ and $\xi_2 = \varepsilon_{n,3}^{cr} / \varepsilon_{n,u}^{cr}$; threshold angle=30º, Poisson's coefficient=0.2; p=2 was assumed to define β in the simulations based on the concept of shear retention factor

Figure 6 compares the force-midspan deflection curves registered experimentally with those obtained numerically. It is verified that adopting the concept of shear retention factor, the numerical model estimates a load carrying capacity higher than the one recorded experimentally, due to the fact that insteade of the shear failure mode observed experimentally, the model predicted a flexural failure mode. However, if a shear softening diagram is used, the model predicts with high accuracy the load carrying capacity of the beams, and the structural softening registered in the experimental tests was also captured in the numerical simulations, inspite of its incapacity of predicting the abrupt load decay occurred in the experimental tests after peak load. Since experimental data to characterize the crack shear softening diagrama are not available the values of τ_p^{cr} and G_f^{II} were estimated from back fitting analysis in order to assure a high precision prediction of the peak load of the tested beams. For the series of f_{cm}=70 MPa, a similar tendency of the numerical simulations was obtained.

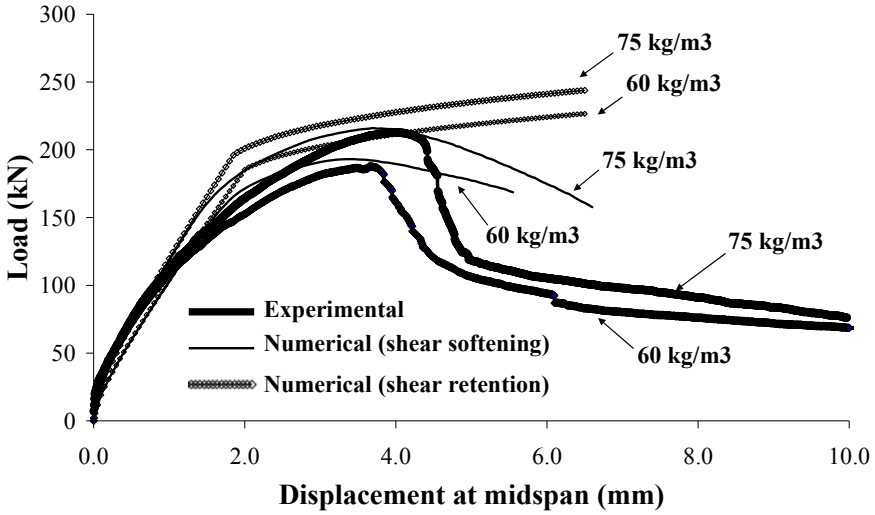

Figure 7 - Relationships between the load and the displacement at the midspan of the RC beams (f_{cm} = 50 MPa)

5. CONCLUSIONS

The experimental program evinced that steel fibre reinforcement provides a significant contribution for the shear resistance of high strength concrete laminar structures. A content of 60 kg/m^3 of hooked end steel fibres of an aspect-ratio of 80 provided an increase on the shear resistance that varied from 80% to 92% for shallow beams of a concrete with an average compressive strength ranging from 50 to 70 MPa. For 75 kg/m^3 of these steel fibres, this increase varied from 102 to 118%.

The formulation proposed by RILEM TC 126 – TDF for the evaluation of the contribution of the fibre reinforcement for the shear resistance of concrete beams provided a safety factor of about 2.26, while a safety factor of 1.92 was obtained in the beams without steel fibres.

The inverse analysis was adopted to determine, indirectly, the values of the mode I fracture parameters of the developed high strength steel fibre reinforced concrete. With these values, and using a softening diagram for modelling the crack shear softening behaviour, a high

accuracy in terms of the load carrying capacity of the tested beams was predicted. This approach was also able of predicting the occurrence of shear failure mode, since after peak load the numerical analysis estimated the development of a structural softening phase. Adopting the conventional concept of shear retention factor for modelling the shear stiffness degradation with the crack opening propagation, a flexural failure mode was predicted, which conducted to ultimate loads higher than the values registered in the experimental tests.

ACKNOWLEDGEMENTS

The authors would like to acknowledge the support provided by FCT by means of the project POCTI/ECM/57518/2004 "FICOFIRE - High performance fiber reinforced concrete of enhanced fire resistance", as well as the collaboration of the Spie Batignolles, Civitest, Secil, Bekaert, Sika and DuroEuropa Companies.

REFERENCES

[1] Swamy, R.N. et al (1993), "Influence of Steel Fibers on the Shear Resistance of Lightweight Concrete I-Beams", ACI Journal, Proceedings V.90, No.1 January-February, pp. 103-114.

[2] Casanova, P., "Bétons de fibres métalliques: du materiau à la structure", PhD Thesis, École Nationale des Ponts et Chaussées, (1995).

[3] RILEM TC 162-TDF, "Test and design methods for steel fibre reinforced concrete - σ ε design method - Final Recommendation", Materials and Structures, Vol.36, October (2003) pp. 560-567.

[4] RILEM TC 162-TDF, "Test and design methods for steel fibre reinforced concrete - σ ε design method - Final Recommendation", Materials and Structures, Vol. 35, (2002) pp. 579-582.

[5] Sena-Cruz, J. M. Et Al, "Stress-crack opening relationship of enhanced performance concrete", 9th Portuguese Conference on Fracture, ESTSetúbal, Portugal, p. 395-403, 18-20 February, 2004

[6] Barros, J.A.O. Et Al, "Post-Cracking Behaviour of Steel Fibre Reinforced Concrete", RILEM Materials and Structures Journal, 38(275), p. 47-56, 2005.